Available online at www.sciencedirect.com

ScienceDirect

IFAC PapersOnLine 50-1 (2017) 2860–2865

Fault detection in airliner electro-mechanical actuators via hybrid particle filtering

M. Mazzoleni *, **G. Maroni** *, **Y. Maccarana** *, **S. Formentin** **, **F. Previdi** *

* *Department of Management, Information and Production engineering University of Bergamo, via Galvani 2, 24044 Dalmine (BG), Italy (e-mail: mirko.mazzoleni@unibg.it).*
** *Department of Electronics, Information and Bioengineering, Politecnico di Milano, via G. Ponzio, 34/5 - 20133 Milano (MI), Italy*

Abstract: In this paper, a modification of the standard particle filter algorithm is applied to face the fault detection issue, on an electro-mechanical actuator. The variant, based on a hybrid system interpretation of the health monitoring problem, is known as OTPF (Observation and Transition Particle Filter). By modeling each fault condition as a hybrid system mode, the method is able to assess the most likely regime for each time stamp. Following this approach, data were acquired from an electro-mechanical actuator, used in aerospace environment, under various fault conditions. The injected mechanical defects consisted in damages undergone by steel spheres, inside a ballscrew transmission system. Then, a model for each condition was identified and the proposed methodology applied. Simulation results show the superiority of the method with respect to the EKF (Extended Kalman Filter), especially because the distribution of the disturbances which affect the system is usually not gaussian.

Keywords: Fault detection and diagnosis; Particle filtering; Diagnosis of discrete event and hybrid systems

1. INTRODUCTION

A fault is defined as a not allowed deviation of at least one system property or parameter, with respect to its nominal operating behaviour, as reported in van Schrick (1997). It is therefore mandatory to equip the system with the ability to report non-standard conditions, detected, usually, by means of a redundancy scheme. Most model-based failure detection and isolation methods rely on the idea of analytical redundancy, see Willsky (1976). In contrast to physical redundancy, the physical sensor is here replaced by a virtual one. This can be beneficial in some applications. The aerospace industry, as an example, places hard constraints on installed equipment volume and weight. A general scheme, introduced by Isermann (2005), highlights the typical components of a model-based fault detection methodology. Faults of different nature can affect both actuators, processes and sensors. Based on system inputs $u(t)$ and outputs $y(t)$, a model of the process under control can then be identified. The feature generation step can be accomplished by one of three different methods:

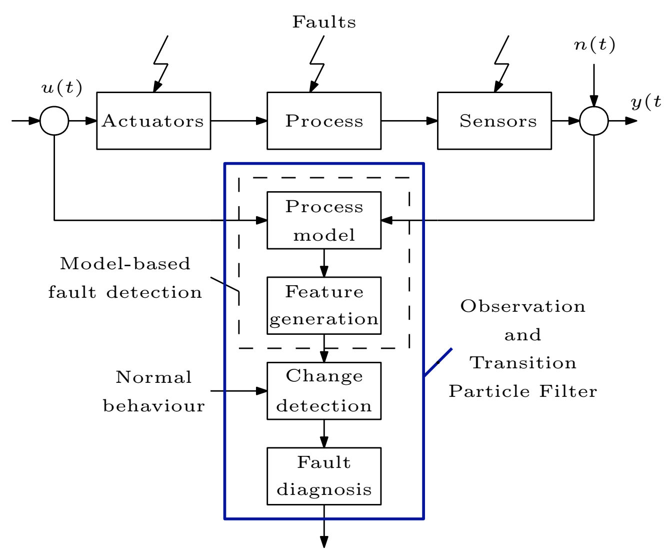

Fig. 1. Classical model-based fault detection scheme, with indication of the OTPF methodology

(1) **Parameter estimation**: the system parameters are computed online with recursive identification algorithms. When the estimated values deviate from the starting ones, a fault is detected. This method is suitable for multiplicative faults, which can be modeled as parameter changes, Isermann (1984)
(2) **State estimation**: the state of the system is estimated via an observer equipped with the nominal model. In this case the detection can be done tracking the behaviour of the state variables and of the observer innovations, Frank and Ding (1997)
(3) **Parity equations**: residuals are computed as $z(t) = y(t) - G(s)u(t)$, where $u(t)$ is the system input, $y(t)$ the measured output and $G(s)$ the process transfer function. These are then subjected to a linear transformation, to obtain the desired fault-detection and isolation properties (see Gertler (1997)). The state estimation and the parity equation methods are suit-

Peer review under responsibility of International Federation of Automatic Control.
10.1016/j.ifacol.2017.08.640

able for additive faults, that influence a variable by the addition of a fault entity.

However, previously described schemes are mostly based on the assumptions that the sytem is linear and affected by gaussian disturbances. Here, the optimal solution to the filtering problem is given by the Kalman filter, and the residuals are represented by its innovations, Willsky (1976). In the case of non-linear systems, sub-optimal solutions are employed, such as the EKF (Extended Kalman Filter). In situations where strong non-linearities or non-gaussian disturbances are present, the EKF method is not able to perfom satisfactorily: algorithms based on the SMC (Sequential Monte Carlo) framework, see Gustafsson (2010), are candidates for employement. The use of these methods in the context of fault detection is not new. Blesa Izquierdo et al. (2015) replaced employed PF (Particle Filter) for fault detection in a sensor network. Koutsoukos et al. (2002) introduced the use of a particle filter algorithm called HBPF (Hybrid Boostrap Particle Filter) for fault detection of hybrid systems. This approach has the disadvantage that faults with low probability of occurring (often the most serious ones) will be harder to detect because less monitored. To solve this problem, Tafazoli and Sun (2006) proposed the OTPF (Observation and Transition Particle Filter). Here, the hybrid system operating mode is interpreted as a particular process status (healthy/faulty). Its estimation permits therefore to solve the detection and diagnosis phase.

The *main contribution* of this paper is the application of the OTPF technique to the fault detection of EMAs (Electro-Mechanical Actuators) deployed for airliners applications. Previous work on model-based fault detection on EMA in aerospace can be found in Balaban et al. (2011); Ismail et al. (2016). The former paper tested various types of mechanical (spalling on raceway, actuator jam) and sensors faults, using a small scale test bed which can be mounted on an aircraft. On the contrary, tests performed during this project are based on a full scale 1:1 scale actuator. In the latter work, authors focused on simulating failures on transmission gears and bearings. Instead, in this work, real faults were injected on an EMA's ballscrew transmission spheres. The employement of the OTPF algorithm in place of the more known EKF is advocated by simulation results. Specifically, when strong non-linearities and non-gaussian disturbances affect the system, the added computational and tuning complexity of the proposed approach is justified. In particular, in aerospace applications, phenomena as atmospheric turbulence (Reeves et al. (1974)) and exhaust plume disturbance (Korona and Kokar (1995)) are typical sources of non-gaussianity.

The remainder of the paper is organized as follows. Section 2 presents the experimental setup deployed for fault injection and data acquisition. Section 3 develops the continous mathematical model of the mechanical system under study. In Section 4, along with a brief description of the standard particle filter method, the OTPF algorithm is described. Section 5 discusses results and comparisons with the Extended Kalman Filter technique, under non-gaussian disturbance distributions simulations. Lastly, Section 6 is devoted to concluding remarks and future developments.

2. EXPERIMENTAL SETUP

The test rig is designed to represent the actuator of primary flight surfaces of a wide-body airliner. With reference to Fig. 2, the EMA is composed by an electric motor and a nut-ballscrew transmission.

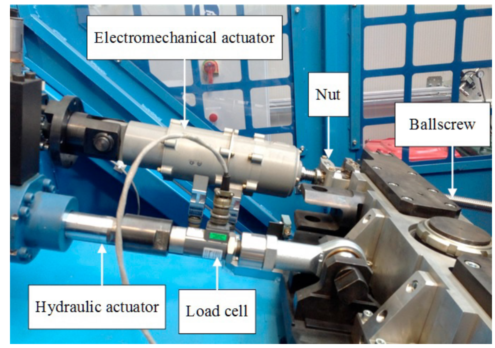

Fig. 2. Test bench components description

The electric motor is a five phases brushless DC motor. This configuration is intrinsically fault tolerant; in fact, the motor performance does not decrease even when two phases are open. The nut contains spheres with a recirculation system and it is moved axially on the screw, transforming the motor rotation into linear movement. More specifically, the nut used in the tests has two recirculation circuits, with 80 spheres per channel, alternating steel and ceramic ones (see Fig. 3).

Fig. 3. Ballscrew transmission detail

A hydraulic system provides the simulated load (mainly due to aerodynamic forces). A load cell measures in real time the delivered load force. A closed loop control system controls the hydraulic system. A complete model of the load system can be found in Cologni et al. (2016), where also the closed loop force control design is shown. Finally, the EMA position is closed loop controlled, ranging from 0 mm (home position) to about 400 mm (fully extended). The fault scenarios investigated in this work are related to sphere damage, in particular steel ball spalling. This kind of fault was chosen as the most significant for this system based on a Fault Tree Analysis (FTA) and a Failure Mode and Effect Analysis (FMEA) performed on the system and here not reported for the sake of brevity. The sphere damage was obtained by an Electrical Discharge Machine (EDM), which removes material providing a truncated sphere shape. In this way, both the shape and the dimension of the spheres are changed. Three level of damage harshness for each sphere have been chosen: light damage (truncated diameter 3.3 mm); medium damage (truncated diameter 3.2 mm); high damage (truncated diameter 3.1 mm). With these spheres damage levels, four different nuts have been prepared for tests:

- Fault 0: no damaged spheres
- Fault 1: 6 damaged spheres (6 light)

- Fault 2: 12 spheres high damaged (6 light; 6 medium)
- Fault 3: 18 spheres high damaged (6 light; 6 medium; 6 high)

Tests were performed in all the described fault conditions, by simply replacing one nut with another. During the measurement tests, the actuator temperature was controlled in order to avoid any temperature-dependent effect. The reference position/speed profile has been defined according to a typical flap full extension and pull back movement. Specifically, during extension the position goes from 0 mm to 411 mm in 20 s with an initial acceleration from 0 mm/s to 21 mm/s in 2 s. During pull back the movement has the same features. The nominal load profile used during the tests corresponds to a typical high lift load profile. In particular, given the actuator position, the load corresponding to that position is applied. Finally, additional constant load profiles at 12 kN and 15 kN where used to test the actuator at load forces close to the maximum design values. Each fault condition was tested repeating twice the aforementioned position/speed profiles with the corresponding load.

3. MODELING

A schematic representation of the developed model is depicted in Fig. 4. The test bench is equipped with two motors but only one is considered for this work, since the other one is disconnected.

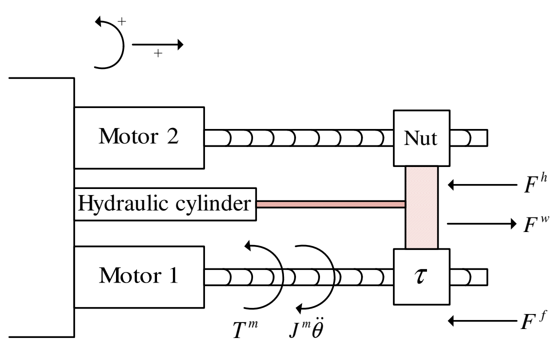

Fig. 4. Diagram of the system dynamic quantities

Indicating with t the continous time, the model inputs consist of:

(1) Motor torque T_t^m - computed by measuring the phase currents
(2) Load force F_t^h - measured from the hydraulic cylinder

The output of the model is:

(1) Motor angular speed $\dot{\theta}_t = \omega_t$ - computed from the position by a resolver

The known parameter is:

(1) Transmission ratio $\tau = \frac{0.005}{2\pi}\left[\frac{\text{m}}{\text{rad}}\right]$
(2) Weight force $F^w = 210\,\text{N}$ - measured experimentally

The unknown parameters are:

(1) Motor inertia J^m
(2) Coulomb f^c, Stribeck f^s, and viscous friction parameters c, c_2, along with the Stribeck velocity ω^s. These coefficients control the friction force F_t^f

Given measured data, a continous time system can be developed and the six parameters identified. From the relations in Fig. 4, it is possible to obtain the following dynamic balance, where the load inertia has been neglected because of the low acceleration of the speed profile used for the performed tests, as discussed in Section 2:

$$T_t^m - J^m\ddot{\theta}_t = \tau\left[F_t^h - F^w + F_t^f\right] \quad (1)$$

The model in Equation 1 can be casted into state-space form by introducing the state variable $x_t = \dot{\theta}_t = \omega_t$:

$$\begin{cases} \dot{x}_t & = \frac{T_t^m - T_t^h + T_t^w - T_t^f}{J^m} \\ y_t & = x_t \end{cases} \quad (2)$$

where T_t^h, T^w, T_t^f are respectively the torques of load, weigth and friction referred to the motor-side. The friction torque, depending on the motor angular speed, is modeled with a Tustin friction model (Armstrong-Hélouvry et al. (1994)):

$$T_t^f = \left[f^c + (f^s - f^c)e^{-\left(\frac{x_t}{\omega^s}\right)^2} + c_2 \cdot (x_t)^2\right] \cdot sign(x_t) + c \cdot x_t \quad (3)$$

Tests were performed at various constant speeds to better characterize the friction behaviour. The quadratic term $c_2(x_t)^2$ has been shown to experimentally better represent the data, as discussed in Niglis and Öberg (2015). In order to simulate the model, the function *sign* has been replaced with the hyperbolic tangent. The model was then discretized using the backward Euler method, in order to implement the filtering procedures described hereafter.

4. FAULT DETECTION VIA PARTICLE FILTERS

4.1 Standard particle filter algorithm

The particle filter (see Arulampalam et al. (2002)) is a special implementation of a SMC method. These techniques make use of simulations to generate weighted samples, that approximate a target distribution. In the context of dynamic systems filtering, this boils down into estimating the state pdf (probability density function). The KF and EKF algorithms estimate the state pdf as a gaussian one: this is correct if the system is linear and the disturbances have normal distribution. The state point estimate is then the mean of that gaussian. In other cases, the employement of SMC algorithms enable the use of samples to compute *any* distribution's moment, and empirically approximate the state pdf, without resorting to a specific distribution's mathematical model. The practical generation of the samples is made possible by the combined actions of importance sampling and resampling schemes, which prevent the *weight degeneracy* issue, Gordon et al. (1993). Consider a generic state-space model, under the usual Markov assumption, where k is the discrete time stamp:

- System model

$$x_k = a(x_{k-1}, e_k) \leftrightarrow \overbrace{f(x_k|x_{k-1})}^{\text{Transition density}} \quad (4)$$

- Measurement model

$$y_k = b(x_k, v_k) \leftrightarrow \overbrace{g(y_k|x_k)}^{\text{Observation density}} \tag{5}$$

Variables x_k and y_k represent respectively the dynamic system state and output, $a(\cdot)$ and $b(\cdot)$ are generic non-linear functions, e_k and v_k are disturbances with known pdf. The system can be equivalently represented by means of the transition and observation densities. The filtering problem consists into estimating the state distribution $\pi_{k|0:k}(x_k|y_{0:k})$ given observations up to time k, assuming that the initial state x_0 is distributed according to $\pi_0(x_0)$. The full state posterior can be obtained by the following recursion, Ho and Lee (1964):

- Prediction

$$\begin{aligned}&\pi_{0:k|0:k-1}(x_{0:k}|y_{0:k-1})\\ &= \pi_{0:k-1|0:k-1}(x_{0:k-1}|y_{0:k-1})\overbrace{f(x_k|x_{0:k-1}, y_{0:k-1})}^{f(x_k|x_{k-1})}\end{aligned} \tag{6}$$

- Correction

$$\pi_{0:k|0:k}(x_{0:k}|y_{0:k}) = \frac{g(y_k|x_k)\pi_{0:k|0:k-1}(x_{0:k}|y_{0:k-1})}{l_{k|0:k-1}(y_k|y_{0_k-1})} \tag{7}$$

where $l_{k|0:k-1}$ is the predictive distribution of y_k given the past observations $y_{0:k-1}$, and $f(x_k|x_{0:k-1}, y_{0:k-1}) = f(x_k|x_{k-1})$ thanks to the Markov property of dynamic systems. For a fixed data realization, this term is a normalising constant. The aim is now to sample from $\pi_{0:k|0:k}(x_{0:k}|y_{0:k})$. Since it is generally impossible to sample directly from this distribution, a sequential version of the importance sampling is employed. Conceptually, N particle paths $\tilde{x}_{0:k}^{(i)}, i = 1 \dots N$ are sampled from a convenient importance distribution $q_{0:k}(x_{0:k}|y_{0:k})$, and the unnormalized importance weights $\tilde{\omega}_k^{(i)}$ are computed:

$$\tilde{\omega}_k^{(i)} = \frac{\pi_{0:k|0:k}(\tilde{x}_{0:k}^{(i)}|y_{0:k})}{q_{0:k}(\tilde{x}_{0:k}^{(i)}|y_{0:k})} \tag{8}$$

Using the weighted sample $\{\tilde{x}_{0:k}^{(i)}, \tilde{\omega}_k^{(i)}\}$, and having normalized the weights, it is possible to compute any distribution's statistic. The trick behind the sequential importance sampling lies in choosing an importance distribution which factorizes as the target posterior distribution (the state pdf). In this way, both particles and weights can be computed recursively. In order to prevent the weights degeneracy problem, a *resampling* scheme is applied to remove particles with low weight and replicate the most important ones. In this work, the state transition density $f(x_k|x_{k-1})$ is chosen as importance distribution: with this choice, new particles are obtained via the system dynamic equations, and weighted according to their likelihood of belonging to the output density (which makes use of the current observation). This algorithm is know as *boostrap particle filter*. For further details and implementation issues, see Cappé et al. (2007).

4.2 Fault detection via particle filters

The idea behind the OTPF method (Tafazoli and Sun (2006)) is to frame the fault detection problem into an hybrid systems formulation (Lygeros et al. (1999)). When, at a certain discrete time instant k, the hybrid system is in the mode $m_k \in \{1 \dots M\}$, with M the number of discrete possible process modes, its behaviour is described by:

$$\begin{cases} x_k &= a_{m_k}(x_{k-1}, e_k) \\ y_k &= b_{m_k}(x_k, v_k) \end{cases} \tag{9}$$

where $a_{m_k}(\cdot)$ and $b_{m_k}(\cdot)$ are generic functions which describe the system dynamics in the mode m_k. It is assumed that the initial mode and initial system state are known. A matrix T, known a-priori, is such that T_{ij} defines the transition probabilities from mode i to mode j. The problem of state estimation in hybrid systems and the fault detection one are strictly interconnected. In fact, assuming that different modes describe the system dynamics against different faults, once the most probable mode at current time is estimated, automatically the detection and identification of the fault are assessed. While much work has been devoted to the filtering of hybrid linear system (see Zhang (1999)), less is known about non-linear models. Proposed solutions to this issue, based on particle filter methods, have been shown to perform well in practice (De Freitas et al. (2004)). In the OTPF method, the hybrid system mode (which can vary at each time stamp) is considered an unknown parameter to be estimated. A step is added to the particle filter procedure to obtain the most likely estimation of the mode from the particles. Once the most probable mode is found, it is assumed that the hybrid system will follow the relative dynamics. Then, the subsequent steps are the same as the standard particle filter. In order to estimate the mode, the OTPF combines the current observation y_k with the mode transition probabilities. This permits to monitor even low occurring modes.

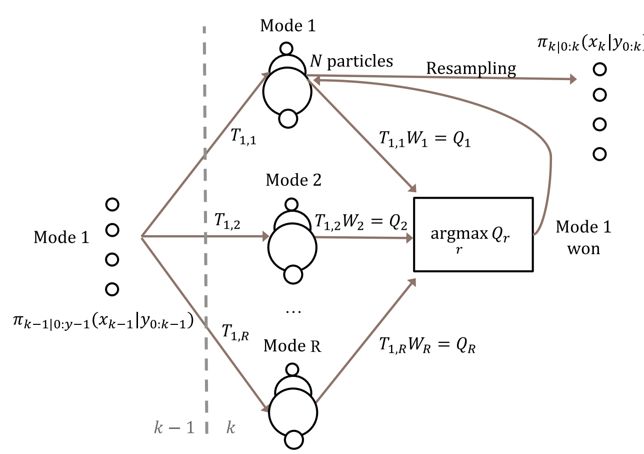

Fig. 5. OTPF single-step procedure

The logic behind the fault detection filtering algorithm, depicted graphically in Fig. 5, is as follows. Given an hybrid system with M possible modes, known process and observation models, N particles are generated from the assumed known initial state. Considering the number R of modes for which the previous mode has not-null transition probability, particles are propagated through each the R modes. The outputs of this step are R sets of N particles. Then, for each mode $r \in \{1 \dots R\}$, the mean weight W_r of all particles in that mode is computed, leveraging on the current measurement y_k. Then, the quantity $Q_r = T_{m_{k-1},r} \cdot W_r$ is computed, with m_{k-1} the selected mode at time $k-1$ and r the hypothesized mode at time k. The mode $m_k = \text{argmax}_r\{Q_r\}$ is chosen as the most plausible one, and its particles resampled and propagated through its dynamic.

5. RESULTS

Data were collected from the test bench described in Section 2. A model, in the form described in Section 4, has been identified for each of the four fault conditions (using data measured with fault injected components), focusing only on the nominal load condition. Simulated data were generated by feeding the four models with the same inputs, and their outputs concatenated. Performances on the fault detection and identification problem are shown, comparing the OTPF with the EKF, under gaussian and uniform distributions. Results show how the OPTF method outperforms the EKF, especially when the noise pdf is not gaussian. The employement of these methods is mandatory given the non-linear form of the models.

The EKF fault detection approach is as follows. The m-th Kalman filter tracks the dynamics of the m-th mode, with $m \in 1, \ldots, M$. The m-th residual at time k is then $z_{k,m} = y_k - \hat{y}_{k,m}$, with y_k the observed output and $\hat{y}_{k,m}$ the predicted output from the mode m filter. If the state estimation is correct, the innovations are gaussian with 0 mean and covariance $\Lambda_{k,m} = [\bar{H}_{k,m} P_{k|k-1} \bar{H}'_{k,m} + V_2]$, where $\bar{H}_{k,m}$ represents the linearized output matrix, $P_{t|t-1}$ is the recursively computed variance matrix of the state prediction error, and V_2 is the covariance of the output disturbances. A fault can be detected by a variation (significative deviation from zero) of the WSR (weighted squared residual): $d_{k,m} = z_{k,m} \Lambda^{-1}_{k,m} z'_{k,m}$. A more robust measure, used in this work, is the WSSR (Weighted Sum Squared Residual): $D_{k,m} = \sum_{j=k-s+1}^{k} d_{j,m}$, where s is the window length in which residuals are added (see Willsky (1976); Zhou et al. (1991)). In the simulations, a value $s = 20$ was chosen. The estimated mode m_k at time k are the one for which the WSSRs are minimum: $m_k = \text{argmin}_m\{D_{k,m}\}$.

5.1 Simulation results

This section reports the simulation results comparing the OTPF with the EKF under different disturbances distributions. The selected number of particles was $N = 100$, while the transition matrix was defined as:

$$T = \begin{bmatrix} 1-\epsilon & \epsilon & 0 & 0 \\ 0 & 1-\epsilon & \epsilon & 0 \\ 0 & 0 & 1-\epsilon & \epsilon \\ 0 & 0 & 0 & 1 \end{bmatrix} \quad (10)$$

where $\epsilon = 10^{-8}$ is chosen as probability of the investigated ballscrew fault, and each column and row reflects the following order: (Fault 0 - Fault 1 - Fault 2 - Fault 3). As an example, $T_{1,2} = \epsilon$ is the probability of transitioning in the "Fault 1" mode, given that the current mode is the "Fault 0" one.

Gaussian disturbances The first experiment added gaussian disturbances to the simulated models states and outputs, both with variance 0.01. The transition and observation densities of the OTPF consisted in gaussian distributions with variance 0.01. The covariances V_1 , V_2 of the state and output noises of the EKFs were set to 0.01. Results are reported in Fig. 6.

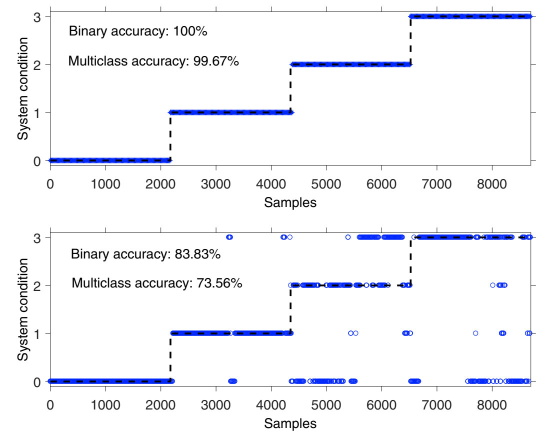

Fig. 6. Fault detection with gaussian disturbances. Top: OTPF estimated system mode (blue dots) vs. real system mode (black dashed line). Bottom: EKF estimation

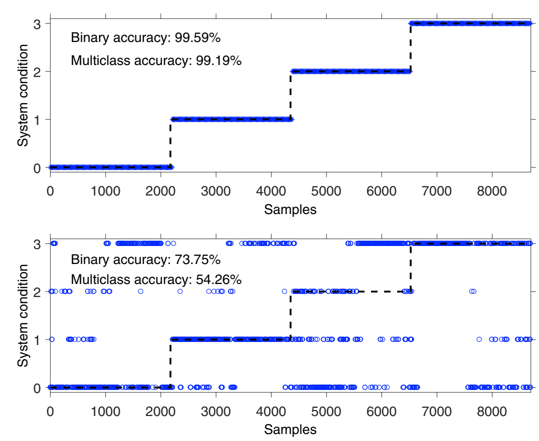

Fig. 7. Fault detection with uniform disturbances. Top: OTPF estimated system mode (blue dots) vs. real system mode (black dashed line). Bottom: EKF estimation

Uniform disturbances The second experiment added disturbances distributed according to an Unif$(-3, 3)$ distribution to the simulated models states, and gaussian noise to outputs, with variance 0.01. The transition density of the OTPF consisted in an Unif$(-3, 3)$ pdf, while the output one was a gaussian with mean 0 and variance 0.01. The covariances V_1 , V_2 of the state and output noises of the EKFs were set to 0.01. Results are reported in Fig. 7.

5.2 Discussion

As it is possible to observe, the OPTF outperforms the EKF in both experiments. While the latter approach still keeps the pace when the disturbances are gaussian, it performs poorly when non-gaussian distribution comes into play. This suggest that, in presence of non standard disturbances and strong non linearities, the employement of a particle filter algorithm can be beneficial. The RMSE (Root Mean Square Error) on the filtering of the state variable was computed for each simulation. Regarding results of Fig. 6, the RMSE for the OPTF was 0.07 while for the EKF was 0.73. As concerns results from Fig. 7, the RMSE for the OPTF was 0.13 while for the EKF was 1.15. For the first experiment, the elapsed time for the OTPF and EKF was 2.27 s and 0.91 s respectively, on a i7-2.30 GHz processor. For the second experiments, the OTPF took 31 s, while the EKF 1.15 s.

6. CONCLUSIONS AND FUTURE DEVELOPMENTS

In this paper, a particle filtering algorithm variant, known as Observation and Transition Particle Filter, has been applied to fault detection of an electro-mechanical actuator. The actuator, deployed in aerospace environments, was injected with real faults on the ballscrew transmission spheres. By collecting data in each fault condition, four different models were identified, where the friction component included a non-linear aspect. The compared non-linear filtering techniques, in terms of fault detection capability, were the OPTF and the EKF methodologies. In order to do this, data were simulated from the four different models. When gaussian noise was added to the data, both techniques performed good. However, when a non-gaussian noise was introduced, the OTPF method clearly won. In aerospace applications, where phenomena such as atmospheric turbulence and exhaust plume disturbance are present, the gaussianity of the disturbances could be a strong assumption. Future research consists of the application of the method on real data and the integration of a model-free approach.

ACKNOWLEDGEMENTS

This research activity has been carried out in the context of the research project *HOLMES* funded by CleanSky Joint Technology Initiative, funding scheme FP7-JTI-CS and Grant Agreement number 338549.

REFERENCES

Armstrong-Hélouvry, B., Dupont, P., and De Wit, C.C. (1994). A survey of models, analysis tools and compensation methods for the control of machines with friction. *Automatica*, 30(7), 1083–1138.

Arulampalam, M.S., Maskell, S., Gordon, N., and Clapp, T. (2002). A tutorial on particle filters for online nonlinear/non-gaussian bayesian tracking. *IEEE Transactions on signal processing*, 50(2), 174–188.

Balaban, E., Saxena, A., Narasimhan, S., Roychoudhury, I., and Goebel, K. (2011). Experimental validation of a prognostic health management system for electro-mechanical actuators. In *Infotech@ Aerospace 2011*, 1518.

Blesa Izquierdo, J., Le Gall, F., Jauberthie, C., and Travé-Massuyès, L. (2015). State estimation and fault detection using box particle filtering with stochastic measurements. In *DX 2015-26th International Workshop on Principles of Diagnosis, 31 August-1 Septembrer, Paris (France)*, 67–73.

Cappé, O., Godsill, S.J., and Moulines, E. (2007). An overview of existing methods and recent advances in sequential monte carlo. *Proceedings of the IEEE*, 95(5), 899–924.

Cologni, A., Mazzoleni, M., and Previdi, F. (2016). Modeling and identification of an electro-hydraulic actuator. In *Control and Automation (ICCA), 2016 12th IEEE International Conference on*, 335–340. IEEE.

De Freitas, N., Dearden, R., Hutter, F., Morales-Menendez, R., Mutch, J., and Poole, D. (2004). Diagnosis by a waiter and a mars explorer. *Proceedings of the IEEE*, 92(3), 455–468.

Frank, P.M. and Ding, X. (1997). Survey of robust residual generation and evaluation methods in observer-based fault detection systems. *Journal of process control*, 7(6), 403–424.

Gertler, J. (1997). Fault detection and isolation using parity relations. *Control engineering practice*, 5(5), 653–661.

Gordon, N.J., Salmond, D.J., and Smith, A.F. (1993). Novel approach to nonlinear/non-gaussian bayesian state estimation. In *IEE Proceedings F-Radar and Signal Processing*, volume 140, 107–113. IET.

Gustafsson, F. (2010). Particle filter theory and practice with positioning applications. *IEEE Aerospace and Electronic Systems Magazine*, 25(7), 53–82.

Ho, Y. and Lee, R. (1964). A bayesian approach to problems in stochastic estimation and control. *IEEE Transactions on Automatic Control*, 9(4), 333–339.

Isermann, R. (1984). Process fault detection based on modeling and estimation methods - a survey. *Automatica*, 20(4), 387–404.

Isermann, R. (2005). Model-based fault-detection and diagnosis–status and applications. *Annual Reviews in control*, 29(1), 71–85.

Ismail, M.A., Balaban, E., and Spangenberg, H. (2016). Fault detection and classification for flight control electromechanical actuators. In *Aerospace Conference, 2016 IEEE*, 1–10. IEEE.

Korona, Z. and Kokar, M.M. (1995). A fusion and learning algorithm for landing aircraft tracking: Compensating for exhaust plume disturbance. *IEEE transactions on aerospace and electronic systems*, 31(3), 1210–1215.

Koutsoukos, X., Kurien, J., and Zhao, F. (2002). Monitoring and diagnosis of hybrid systems using particle filtering methods. In *International Symposium on Mathematical Theory of Networks and Systems*.

Lygeros, J., Tomlin, C., and Sastry, S. (1999). Hybrid systems: modeling, analysis and control. *preprint*.

Niglis, A. and Öberg, P. (2015). Modelling high-fidelity robot dynamics.

Reeves, P.M., Campbell, G., Ganzer, V., and Joppa, R. (1974). Development and application of a non-gaussian atmospheric turbulence model for use in flight simulators.

Tafazoli, S. and Sun, X. (2006). Hybrid system state tracking and fault detection using particle filters. *IEEE Transactions on Control Systems Technology*, 14(6), 1078–1087.

van Schrick, D. (1997). Remarks on terminology in the field of supervision, fault detection and diagnosis. In *Preprints of the 3rd IFAC Symposium on Fault Detection, Supervision and Safety for Technical Processes SAFEPROCESS*, 959–964.

Willsky, A.S. (1976). A survey of design methods for failure detection in dynamic systems. *Automatica*, 12(6), 601–611.

Zhang, Q. (1999). Optimal filtering of discrete-time hybrid systems. *Journal of Optimization Theory and Applications*, 100(1), 123–144.

Zhou, D., Xi, Y., and Zhang, Z. (1991). Non-linear adaptive fault detection filter. *International journal of systems science*, 22(12), 2563–2571.